

Evaluation of Module Dynamics in Functional Brain Networks After Stroke*

Kaichao Wu^{1,2}, Qiang Fang¹, Katrina Neville² and Beth Jelfs³

Abstract—The brain’s functional network can be analyzed as a set of distributed functional modules. Previous studies using the static method suggested the modularity of the brain function network decreased due to stroke; however, how the modular network changes after stroke, particularly over time, is far from understood. This study collected resting-state functional MRI data from 15 stroke patients and 15 age-matched healthy controls. The patients exhibit distinct clinical symptoms, presenting in mild ($n = 6$) and severe ($n = 9$) subgroups. By using a multilayer network model, a dynamic modular structure was detected and corresponding interaction measurements were calculated. The results demonstrated that the module structure and interaction had changed following the stroke. Importantly, the significant differences in dynamic interaction measures demonstrated that the module interaction alterations were not independent of the initial degree of clinical severity. Mild patients were observed to have a significantly lower between-module interaction than severe patients as well as healthy controls. In contrast, severe patients showed remarkably lower within-module interaction and had a reduced overall interaction compared to healthy controls. These findings contributed to the development of post-stroke dynamics analysis and shed new light on brain network interaction for stroke patients.

Clinical relevance—Dynamic module interaction analysis underpins the post-stroke functional plasticity and reorganization, and may enable new insight into rehabilitation strategies to promote recovery of function.

I. INTRODUCTION

After a stroke, the brain adjusts its functional network connectivity to adapt to the physical damage and to compensate for lost function [1], [2]. The human brain consists of functionally specialized modules, that is, brain regions within modules and between modules which interact in response to the functional demands of the external environment [3]. Therefore, the altered functional connectivity after stroke implies changes in this cooperation or interaction within or between functional modules.

The modular functional network can be assessed by modularity, which is a measure of how well the division of the network into smaller modules describes the structure of

*This work was supported by Li Ka Shing Foundation Cross-Disciplinary Research Grant (2020LKSFG01C).

¹Kaichao Wu and Qiang Fang are with the Department of Biomedical Engineering, College of Engineering, Shantou University, Shantou, China {kaichao.wu, qiangfang}@stu.edu.cn).

²Kaichao Wu and Katrina Neville are with the School of Engineering, RMIT University, Melbourne, Australia katrina.neville@rmit.edu.au.

³Beth Jelfs is with the Department of Electronic, Electrical, and Systems Engineering, University of Birmingham, Birmingham, UK. b.jelfs@bham.ac.uk.

the network [4]. Previous studies have frequently reported reduced modularity of functional networks after strokes [5], [6], which can to some extent, explain the post-stroke clinical deficits [7]. The reduction of modularity proves alteration of the post-stroke functional module; however, how brain regions interact within or between the functional modules, leading to the decreased modularity, is not clear. In addition, previous findings basically rested on single or static functional networks built from entire resting-state functional MRI signals. While static implementation is effective and fruitful, increasing recognition of temporal dynamics suggests that the functional module, particularly its inter- and intra-interaction, varies over time, thus emphasizing the need to characterize these dynamic changes [8], [9].

To address the above, functional module dynamics in stroke patients were evaluated for the first time in this study, using a multilayer network model. We analyzed resting-state fMRI in 15 stroke patients (6 mild, and 9 severe) and 15 age-matched healthy controls. We hypothesized that the functional modules in the brain network are significantly altered after the stroke, exhibiting a different number of time-varying modules and temporally distinct module interaction trajectories. To test this hypothesis, three dynamic module interaction measures were calculated, and we observe that these measurements are not independent of the clinical symptoms, i.e., mild and severe patients exhibit different interaction patterns.

II. MATERIALS AND METHODS

A. Participants

Stroke samples examined in this study were from fifteen ischemic stroke patients admitted to the 1st affiliated hospital of Shantou University Medical College (SUMC) (4 males and 11 females, the mean day post-stroke of the MRI scan is 23.06 with a standard deviation of 4.32). Six and nine patients were assigned to the mild and severe subgroups according to clinical NIHSS(the national institutes of health stroke scale) scores, respectively. Fifteen age-matched healthy participants served as control groups (7 males and 8 females, mean age is 68.6 with a standard deviation of 6.4 years). The patients were recruited from a study approved by the medical research ethics committees of the named hospital, and all participants signed informed consent.

B. fMRI Acquisition and Pre-Processing

Acquisition of MRI data was performed on a Discovery standard 3.0 T scanner using an 8-channel head coil at

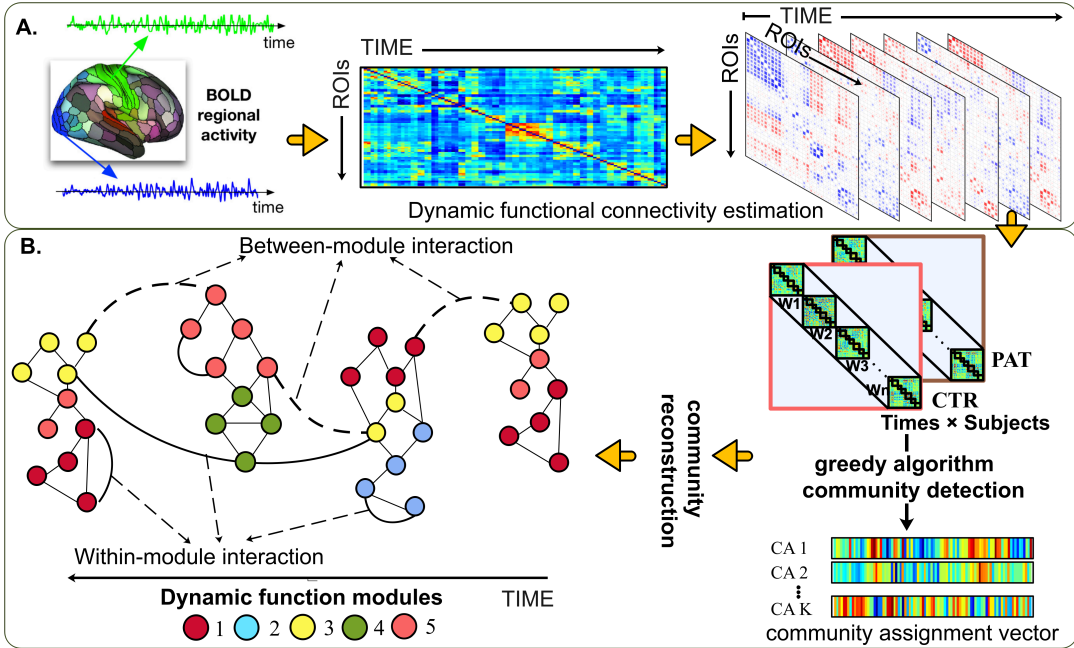


Fig. 1. Flowchart of the proposed analytical framework. **A.** Dynamic functional connectivity estimation. **B.** Dynamic module interaction analysis. The arrows indicate the direction of data flow.

the MRI centre of SUMC. The high-resolution T1 anatomical images were acquired with a multi-planar rapidly acquired gradient echo sequence. Resting-state functional MRI was collected after the anatomical scan using single-shot gradient-echo EPI sequence: repetition time (TR) = 2,000 ms; echo time = 30 ms; voxel size = $3.43 \times 3.43 \times 5.0 \text{ mm}^3$ with no gap; 210 volumes acquired in 7 min.

The fMRI data were processed using a customized pre-processing pipeline in the CONN functional connectivity toolbox [10] in conjunction with the Statistical Parametric Mapping software package (SPM12). For all participants, the first 10 dummy functional volumes were removed. The remaining images were corrected for slice timing and head motion and normalized to Montreal Neurologic Institute (MNI) space. Non-smoothed functional images were then fed into the default denoising pipeline, for confounding effect elimination and temporal band-pass filtering (0.008–0.09 Hz).

C. Dynamic Functional Connectivity Estimation

Fig. 1 outlines our proposed analytic framework, as can be seen the first component in the analysis is dynamic functional network connectivity (dFNC) estimation. In this work, the regions of interest (ROIs) were recognized by using a functional brain parcellation provided by CONN (32 regions forming eight large-scale networks) [10]. The regional BOLD timeseries were extracted from the denoised fMRI data, then dFNC was estimated by using a sliding window approach. We used a tapered window, which was obtained by convolving a rectangle (equal to the window size) with a Gaussian ($\sigma = 3$) at each time point. The window width is 50 TR and the shifting with a step of 1 TR [9], resulting in 151 total windows. At each window, a $N \times N$ functional connectivity matrix A was created with

N ROIs, where each entry A_{ij} is the Pearson's coefficient between pairwise timeseries of ROI i and j . Finally, Fisher's Z-transformation was applied to eliminate the bias, with only the positive values being retained in the subsequent analysis.

D. Dynamic Functional Module Estimation

From the dynamic functional connectivity estimates, the dynamic functional modules can be estimated as follows. First, the estimated dFNC of all participants (both stroke patients and healthy controls) were concatenated along a matrix diagonal to produce their initial community profile (the size is equal to the number of sliding windows times the size of each window). Then, the Louvain-like greedy community algorithm was used for dynamic module detection. This algorithm optimizes the multilayer modularity partition by maximizing the modularity quality function [11] which is defined as:

$$Q_M = \frac{1}{2\mu} \sum_{ijlr} \left[\left(A_{ijl} - \gamma \frac{k_{il}k_{jl}}{2m_l} \right) \delta_{lr} + \delta_{ij} \omega_{lr} \right] \delta(g_{il}, g_{jr}), \quad (1)$$

$$Y = m \times \log(t) + b, \quad (2)$$

where μ is the sum of the weights of the dynamic functional connectivity matrix A across all nodes i and j and layers l and r ; k_{il} and k_{jl} are the weighted degrees of nodes i and j at layer l , and m_l is the total nodal weighted degrees; $\delta_{ij} = 1$ if $i = j$, otherwise 0. g_{il} and g_{jr} represent the community assignment of the node i in layer l and the community assignment of the node j in layer r respectively. $\delta(g_{il}, g_{jr}) = 1$ if $g_{il} = g_{jr}$, otherwise 0. The parameters γ and ω are the intra-layer and inter-layer coupling parameters, where $\gamma = 0.9$ and $\omega = 1.0$ [9].

The final result of this optimization is the functional connectivity modularity associated with each sliding window. Hence, for the 151 dFNC estimates for each subject, there would be 151 community assignment vectors; each one indicating the module the ROIs are assigned to. After reconstruction, a multilayer network with a complex and rich module structure spanning the time-varying layers is obtained.

E. Dynamic module analysis

With the dynamic modules estimated, the number of unique modules, the between-module interaction and the within-module interaction can be calculated. The between-module interaction, BI_t , measures to what extent nodes from a module interact with nodes from another module, and is defined as:

$$BI_t = \frac{1}{|C|} \sum_c^C \sum_{i \in c}^n \sum_{j \notin c}^n A_{ijt}, \quad (3)$$

where C is the detected number of modules, $|C|$ is the number of detected modules that have at least one connectivity at layer t . Likewise, the nodes in a module that interact with each other is measured by the within-module interaction WI_t , which is defined as:

$$WI_t = \frac{1}{|C'|} \sum_c^C \sum_{i \in c}^n \sum_{j \in c}^n A_{ijt}, \quad (4)$$

where $|C'|$ is the number of detected modules where at least two nodes of the module have one connectivity at layer t .

In addition, an overall interaction coefficient, IC , was proposed to measure the trade-off of the between-module interaction and the within-module interaction:

$$IC = \frac{\overline{WI} - \overline{BI}}{\overline{WI}} \quad (5)$$

Where \overline{WI} represents the average strength of all within-module interactions across time and \overline{BI} is the average strength of all between-module interactions across time.

F. Statistical Analysis

A three-level one-way ANOVA (level of significance $p < 0.05$, false discovery rate (FDR) corrected) was performed to investigate if there were statistically significant differences in module interaction between healthy controls and mild and severe patients. In case of significant ANOVA results, post hoc t-tests (mild vs. severe, severe vs. controls, and mild vs. controls) were performed.

III. RESULTS

A. Detected Module Structure

As Fig. 2 shows, there was a significant difference in the number of dynamic modules formed ($F = 4.68$, $p < 0.05$). A post-hoc t-test reveals that mild stroke patients have significantly fewer modules than healthy controls. There was no significant difference between mild and severe patients, nor between severe patients and the control group. Note that since the dynamic module was estimated across the

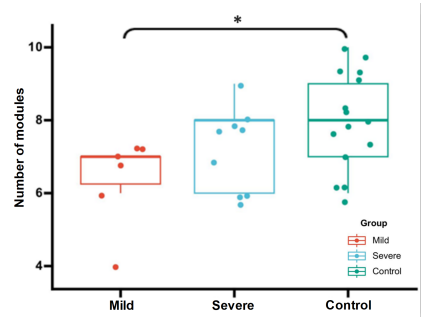


Fig. 2. Differences between subgroups in the number of detected modules (* $p < 0.05$, FDR corrected). Boxplots represent the median and interquartile range.

layers, the module number at each layer does not equal the total number of detected modules. Fig. 3A) displays the dynamic change in the number of modules over time for all 30 participants. For all participants, the number of modules at each layer is no more than 4, however, the module that ROIs are assigned exhibits differences. For example, the right precuneus cortex (PCC) and left precuneus cortex (SMG) of patient 5, at layers 40 and 75, have distinct community assignments (the colour bar indicates their functional module).

B. Module Interaction Over Time

Fig. 3B shows the time course of the module interaction over time for each group. As can be seen the curves of the within-module and between-module interactions for both the mild and severe stroke patients are lower than the healthy controls; this trend was not apparent for the between-module interactions of severe patients in the middle and later periods of the MRI scan. Interestingly, the between-module interaction of mild and severe patients exhibited the opposite trend of within-module interaction. The mild patients mostly had greater within-module interaction than the severe patients, while in the between-module interaction, they were much lower than severe patients.

C. Module Interaction Between Different Levels of Stroke Severity

Fig. 3C shows the group effect for module interaction. One-way ANOVA analysis revealed significant differences in all three interaction measures (within-module interaction: $F = 3.48$, $p < 0.05$; between-module: $F = 4.32$, $p < 0.05$; and coefficient: $F = 3.75$, $p < 0.05$). A post-hoc t-test showed that severe patients have significantly lower within-module interaction ($p = 0.041$) and overall interaction coefficient ($p = 0.018$) than healthy controls. While no significant differences were detected in within-module interaction and interaction coefficient between mild patients and controls, mild patients were observed to have much lower between-module interaction than severe patients ($p = 0.0048$) and lower than controls ($p = 0.018$).

IV. DISCUSSION

This study performed a dynamic module analysis on stroke patients for the first time. The temporally variable functional

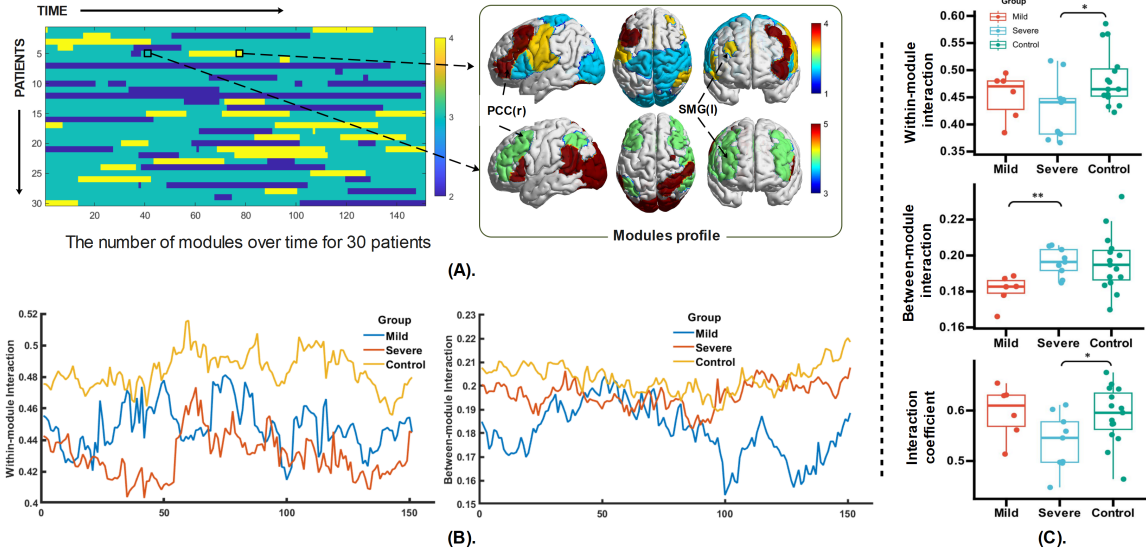


Fig. 3. Dynamic module analysis results: **A.** The number of modules over time for 30 patients. **B.** The trajectory of module interaction over time. **C.** Between group comparison of dynamic module interaction measures (** $p < 0.01$, * $p < 0.05$, FDR corrected).

modules identified are formed by a subset of brain regions that are highly interactive with one another and less interactive with other subsets of brain regions. The significant differences in the number of modules across groups indicate that the functional structure has changed after the stroke. Mild patients tend to have a more compact module structure than healthy controls, which supports the findings that modularity is reduced after stroke [6]. In addition, following the time course of the module interaction, we found that, compared with healthy controls, stroke patients generally show lower within-module and between-module interaction over time. Notably, the time courses of the two module interactions exhibit opposite trends for the mild stroke patients compared to the severe stroke patients, suggesting module interaction could potentially be a new biomarker for stroke severity [12].

In addition, we found that mild patients exhibit significantly lower between-module interaction than severe patients and healthy controls. Whereas no differences were observed in within-module interaction or overall interaction. In contrast, severe patients showed a remarkably lower within-module interaction and a reduced overall interaction compared to healthy controls; no differences were observed in between-module interaction. These findings demonstrated that stroke patients' interaction patterns diverged from those of healthy controls depending on their clinical severity [13].

Furthermore, the overall interaction coefficient concerns a concept of functional segregation [14] (the degree that the formed functional modules prefer to interact with others). The severe patients showed significantly lower overall interaction, implying that the functional systems or domains in the brains of severe stroke patients tend to process information in smaller islands of isolation [13], [15].

V. CONCLUSION

The present study explored the post-stroke module dynamics in the functional brain network. The time-varying

modules in stroke patients diverge from those of healthy control, depending on their clinical symptoms. This is the first attempt to investigate the alteration in dynamic module structure and interaction caused by stroke. It provides a novel exploration of the dynamic method applied in the stroke and offers insight into temporal dynamics engaged in post-stroke plasticity and reorganization.

REFERENCES

- [1] M. H. Adhikari *et al.*, "Decreased integration and information capacity in stroke measured by whole brain models of resting state activity," *Brain*, vol. 140, no. 4, pp. 1068–1085, 2017.
- [2] E. Carrera and G. Tononi, "Diaschisis: past, present, future," *Brain*, vol. 137, no. 9, pp. 2408–2422, 2014.
- [3] O. Sporns and R. F. Betzel, "Modular brain networks," *Annu. Rev. Psychol.*, vol. 67, p. 613, 2016.
- [4] M. E. Newman, "Modularity and community structure in networks," *Proc. Natl. Acad. Sci.*, vol. 103, no. 23, pp. 8577–8582, 2006.
- [5] E. S. Duncan and S. L. Small, "Increased modularity of resting state networks supports improved narrative production in aphasia recovery," *Brain Connect.*, vol. 6, no. 7, pp. 524–529, 2016.
- [6] C. Grattan *et al.*, "Focal brain lesions to critical locations cause widespread disruption of the modular organization of the brain," *J. Cogn. Neurosci.*, vol. 24, no. 6, pp. 1275–1285, 2012.
- [7] J. S. Siegel *et al.*, "Re-emergence of modular brain networks in stroke recovery," *Cortex*, vol. 101, pp. 44–59, 2018.
- [8] D. J. Lurie *et al.*, "Questions and controversies in the study of time-varying functional connectivity in resting fMRI," *Netw. Neurosci.*, vol. 4, no. 1, pp. 30–69, 2020.
- [9] Z. Yang *et al.*, "Measurement reliability for individual differences in multilayer network dynamics: Cautions and considerations," *NeuroImage*, vol. 225, p. 117489, 2021.
- [10] S. Whitfield-Gabrieli and A. Nieto-Castanon, "CONN: a functional connectivity toolbox for correlated and anticorrelated brain networks," *Brain Connect.*, vol. 2, no. 3, pp. 125–141, 2012.
- [11] P. J. Mucha *et al.*, "Community structure in time-dependent, multi-scale, and multiplex networks," *Science*, vol. 328, no. 5980, pp. 876–878, 2010.
- [12] F. Vecchio *et al.*, "Cortical connectivity from EEG data in acute stroke: A study via graph theory as a potential biomarker for functional recovery," *Int. J. Psychophysiol.*, vol. 146, pp. 133–138, 2019.
- [13] A. K. Bonkhoff *et al.*, "Acute ischaemic stroke alters the brain's preference for distinct dynamic connectivity states," *Brain*, vol. 143, no. 5, pp. 1525–1540, 2020.

- [14] S. B. Eickhoff and C. Grefkes, “Approaches for the integrated analysis of structure, function and connectivity of the human brain,” *Clin. EEG Neurosci.*, vol. 42, no. 2, pp. 107–121, 2011.
- [15] A. K. Bonkhoff *et al.*, “Abnormal dynamic functional connectivity is linked to recovery after acute ischemic stroke,” *Hum. Brain Mapp.*, vol. 42, no. 7, pp. 2278–2291, 2021.